THE ASTROPHYSICAL JOURNAL, 408:L25–L28, 1993 May 1

THE FREEZE-OUT PHASE OF SN 1987A: IMPLICATIONS FOR THE LIGHT CURVE

CLAES FRANSSON AND CECILIA KOZMA
Stockholm Observatory, S-133 36 Saltsjöbaden, Sweden
Received 1992 October 30; accepted 1993 February 8

ABSTRACT

After ~800 days, time-dependent effects due to long recombination and cooling times lead to a frozen-in structure of the ejecta of SN 1987A. The result is a higher bolometric luminosity, compared to models where the emitted luminosity is equal to the instantaneous energy input. Good agreement with the observed light curve of SN 1987A is obtained with an initial $^{57}Ni/^{56}Ni$ ratio 2 times the solar $^{57}Fe/^{56}Fe$ ratio, while steady state models require a factor of 2 more. Consistency with both the ^{57}Co mass from IR line observations, X-ray, and γ-ray observations, and from models of the nucleosynthesis can thus be obtained.

Subject headings: nuclear reactions, nucleosynthesis, abundances — supernova remnants — supernovae: individual (SN 1987A)

1. INTRODUCTION

Late observations of SN 1987A are of special interest for both the nucleosynthesis and eventual effects of a neutron star (see Chevalier 1992 for a recent review). Analysis of the light curve and the spectrum indicate that the evolution has entered a new phase. The light curve shows a less rapid decline than expected from pure ^{56}Co excitation (Bouchet, Danziger, & Lucy 1991; Suntzeff et al. 1991, 1992; Menzies 1991). Spectroscopic observations after day 700 reveal a clear flattening of the fluxes in all lines (Danziger et al. 1991; Suntzeff et al. 1991; Menzies 1991), as well as an increase in the widths of many of the lines. By these authors and others (Kumagai et al. 1991; Woosley, Pinto, & Hartmann 1989), the flattening of the light curve has been interpreted alternatively as a sign of new radioactive isotopes with longer decay time scales, or an additional energy source, presumably a neutron star. The most likely isotopes are ^{57}Co and ^{44}Ti, and based on the bolometric light curve, a ratio $^{57}Ni/^{56}Ni$ corresponding to $^{57}Fe/^{56}Fe$ 5 times solar has been claimed (Suntzeff et al. 1991, 1992). This conflicts with the value 1.5 times solar determined spectroscopically from [Fe II] and [Co II] IR lines (Danziger et al. 1991; Varani et al. 1990), and in particular with the OSSE observation of the 122 keV ^{57}Co line (Kurfess et al. 1992). Additional evidence for a new phase comes from modeling of the Hα evolution (Kozma & Fransson 1992, hereafter Paper I), which predicts considerably lower fluxes after ~800 days than observed. Finally, Woosley & Hoffman (1991) find that not more than 2.5 times the solar ratio can be produced without severe difficulties in reproducing other iron group isotopes.

Until now, all models and claims for extra energy input have been based on the assumption of instantaneous conversion of the absorbed γ-ray, or positron, energy into radiation, i.e., that the plasma is in ionization and thermal equilibrium. In this *Letter* we show that this is not justified. After this *Letter* was submitted, the effect of a frozen-in ionization was also independently suggested by Clayton et al. (1992), using a simplified model with only hydrogen and without temperature effects.

2. FREEZE-OUT

Gamma rays emitted in the radioactive decay are Compton-scattered in the remnant, producing a population of fast, secondary electrons. These are slowed down by ionizations, excitations, and elastic Coulomb scatterings in the gas (Paper I and references therein). Most of the ionization energy is emitted as recombination emission, while Coulomb scatterings heat the plasma. Heating is balanced by collisional excitation cooling. A requirement for steady state is therefore that the recombination time scale, t_{rec}, and the cooling time scale, t_{cool}, are short compared to the radioactive decay time scale, τ_{decay}, and the expansion time scale t. For ^{56}Co, $\tau_{decay} = 111.26$ days, and for ^{57}Co $\tau_{decay} = 391$ days. For epochs of interest these time scales are both shorter than the expansion time scale. Therefore, the steady state requirement is that max (t_{rec}, t_{cool}) $\ll \tau_{decay}$. If the cooling time scale should become longer than the expansion time scale, adiabatic cooling has to be included. Both t_{rec} and t_{cool} are functions of temperature and the state of ionization and should be calculated from detailed ionization models (§ 3). As an illustrative example, we consider the recombination of the H component in the core.

Based on the line widths, most Hα emission is coming from gas with velocities less than ~3000 km s^{-1} (e.g., Danziger et al. 1991). Hydrodynamic simulations (Fryxell, Müller, & Arnett 1991; Nomoto et al. 1993; Herant & Benz 1992) show that hydrogen penetrates deep into the core, and we assume that this component has a filling factor ϵ and mass $M(\mathrm{H})_{core}$. From Fryxell et al. we find $\epsilon \sim 0.4$ and $M(\mathrm{H})_{core} \sim 1\ M_\odot$, while Nomoto et al. and Herant & Benz find $M(\mathrm{H})_{core} \sim 2\ M_\odot$. After ~500 days, ionization of H I is dominated by nonthermal ionizations from the ground state. The effective ionization potential of H I is ~37 eV in the range $x_e = 10^{-3}$ to 10^{-2} (Paper I). The electron fraction, x_e, in the H-rich gas is then given by

$$x_e = 0.22\epsilon^{1/2} D_\gamma^{1/2} \left[\frac{M(^{56}\mathrm{Ni})}{0.07\ M_\odot}\right]^{1/2} \left(\frac{V_{core}}{2000\ \mathrm{km\ s^{-1}}}\right)^{1/2} \times \left(\frac{M(\mathrm{H})_{core}}{1\ M_\odot}\right)^{-1/2} \left(\frac{T_e}{5000\ \mathrm{K}}\right)^{0.4} \left(\frac{t}{1000^{\mathrm{d}}}\right)^{1/2} e^{-t/222^{\mathrm{d}}}.$$

Here we approximate the γ-deposition factor by $D_\gamma = (1 - e^{-\tau_\gamma})/\tau_\gamma$, where τ_γ is the total effective γ-ray optical depth. For $t > 700$ days, $\tau_\gamma < 1$, and $D_\gamma \approx 1$. The temperature dependence comes from $\alpha_{rec} = 4.5 \times 10^{-13}(T_e/5000\ \mathrm{K})^{-0.8}$ cm^3 s^{-1} (case B). Using $t_{rec} = 1/\alpha_{rec} n_e$, and $T_e \approx 5000$ K, we find for

^{56}Co that $t_{rec} \approx \tau_{decay}$ at t_{freeze}, given implicitly by

$$t_{freeze} = 980 + 222\left[\left[\frac{1}{2}\ln\left\{\left(\frac{\epsilon}{0.4}\right)^{-1}\left[\frac{M(^{56}\mathrm{Ni})}{0.07\ M_\odot}\right]\left[\frac{M(\mathrm{H})_{core}}{1\ M_\odot}\right]\right\} - \frac{5}{2}\ln\left[\left(\frac{V_{core}}{2000\ \mathrm{km\ s^{-1}}}\right)\left(\frac{t_{freeze}}{980^d}\right)\right]\right] \mathrm{days}\ .$$

After $\{1275 - 155.6 \ln [M(^{57}\mathrm{Ni})/(1.8 \times 10^{-3}\ N_\odot)]\}$ days, ^{57}Co input dominates ^{56}Co, where we have normalized $M(^{57}\mathrm{Ni})$ to a solar ^{57}Fe/^{56}Fe ratio, and set $M(^{56}\mathrm{Ni}) = 0.07\ M_\odot$. t_{freeze} is then given by a similar expression, with 980 days, 222 days and $[M(^{56}\mathrm{Ni})/0.07\ M_\odot]$ replaced by 1158 days, 782 days and $[M(^{57}\mathrm{Ni})/(1.8 \times 10^{-3}\ M_\odot)]$, respectively. After t_{freeze} the state of ionization is essentially frozen in. t_{freeze} depends on the density structure, the composition, and whether ^{56}Co or ^{57}Co input dominates. Most of these dependencies enter logarithmically, and the above estimate should be fairly insensitive to the structure of the remnant. In the envelope t_{freeze} is reached earlier. If we approximate the envelope density profile as a function of velocity, V, by $\rho(V) \propto V^{-n}$, with $n \approx 1$–2, one finds $t_{rec} \propto V^{(1+n/2)}$. Therefore, freeze-out first sets in at high velocities and gradually moves inward.

Based on these considerations we conclude that *after* t_{freeze} *the evolution of the emission from the supernova must be calculated by a self-consistent, time-dependent method. A quasi-steady approximation underestimates both the level of ionization and the emission from the ejecta.* After t_{freeze} the ionization is essentially constant. Luminosities of both collisional excited and recombination lines are proportional to $\int n n_e dV \propto t^{-3}$ and are expected to decrease as t^{-3}, much slower than the radioactive decay time scale. Since most of the emission comes out as line radiation, we expect the bolometric light curve to behave in a similar way. In § 3 we find that adiabatic cooling dominates the radiative cooling in the H and He components after ~1000 days, and in the envelope even earlier. Temperature then decreases as $T_e \propto t^{-2}$, further decreasing the collisional line emission. In the O core, cooling is more efficient.

3. BOLOMETRIC LIGHT CURVES

To verify this picture quantitatively, we have calculated the evolution of the temperature and ionization of the ejecta, using a time-dependent ionization/recombination code. We include H, He, C, N, O, Ne, Mg, Si, Ca, and Fe, each with neutral and singly ionized stages. H I, He I, O I, and Ca II are treated as multilevel atoms with 6, 16, 10, and 4 levels, respectively, including the continuum, with the line transfer treated by the Sobolev method. Photoionization by line emission and the two-photon continua of H I and He I are included. Molecular cooling, which may be important in the core (Liu, Dalgarno, & Lepp 1992), is not included. We hope to discuss this in a future paper (Kozma & Fransson 1993, hereafter Paper III). The temperature and ionization of the three primary composition regions in the core and envelope (see below) are calculated separately. The ionization, level populations and temperature are calculated time dependently, using an implicit method. Atomic data are discussed in Fransson & Chevalier (1989) and in Paper III. The calculation is started at 400 days, before time-dependent effects become important. Energy conservation has been checked carefully and found to be satisfied within 20% at all times, and within 5% later than 700 days.

Nonthermal excitation, ionization, and heating rates are taken from Paper I. From the bolometric light curve we set $M(^{56}\mathrm{Ni}) = 0.07\ M_\odot$. In our standard case we include ^{57}Ni with ^{57}Ni/^{56}Ni equal to 2 times the solar ^{57}Fe/^{56}Fe ratio, or $3.3 \times 10^{-3}\ M_\odot$, and discuss variations of this below. Because of the lower mean energy of the γ-rays, the effective opacity for the ^{57}Co γ-rays is 2.4 times larger than for ^{56}Co (Woosley et al. 1989). We also include γ-ray input from ^{44}Ti and positrons due to ^{56}Co and ^{44}Ti. Only ^{44}Ti positron input is important, with $L_+ = 9.9 \times 10^{35}[M(^{44}\mathrm{Ti})/10^{-4}\ M_\odot]$ ergs s^{-1}. Most γ-rays have energies of 511 keV or 1.157 MeV, and we use the same opacity as for ^{56}Co, and a total luminosity $L_\gamma = 4.0 \times 10^{36}[M(^{44}\mathrm{Ti})/10^{-4}\ M_\odot]$ ergs s^{-1}. The ^{56}Co and ^{44}Ti positrons have an average energy of ~600 keV. Using the Bethe stopping power formula with a mean excitation energy of 275 eV, appropriate to Fe (Ahlen 1980), we estimate a stopping power of ~1.5 MeV cm^2 g^{-1}, and a range of ~0.2 g cm^{-2}. In terms of the core radius, the positrons will propagate a distance

$$\frac{\Delta r}{R_{core}} = 3 \times 10^{-2}\left(\frac{M_{core}}{4\ M_\odot}\right)^{-1}\left(\frac{V_{core}}{2000\ \mathrm{km\ s^{-1}}}\right)^2\left(\frac{t}{1000\ \mathrm{days}}\right)^2,$$

and will be thermalized essentially "on the spot," *even without* a magnetic field. Consequently, we assume that the positron input takes place only in the metal-rich clumps in the core. Although the ^{44}Ti mass calculated by Woosley, Pinto, & Weaver (1988), (0.57–1.3) $\times 10^{-4}\ M_\odot$, agrees well with that found by Kumagai et al. (1991), $1.2 \times 10^{-4}\ M_\odot$, Woosley & Hoffman (1991) argue that the range could be as large as 10^{-6} to $10^{-4}\ M_\odot$, scaling roughly inversely with density. Our standard case has $M(^{44}\mathrm{Ti}) = 10^{-4}\ M_\odot$.

To keep the calculation manageable, but still realistic, we use a simplified form of the density and composition structure. To simulate the macroscopic mixing in the core, we assume in the center a 6 $M_\odot$ core with three components distributed in a shell around the central "Ni-bubble" and expanding with a representative velocity 1500 km s^{-1}. Each component therefore has a constant density, $\rho = 3M_i/(4\pi\epsilon_i V_{core}^3 t^3)$. Specifically, the shell consists of 2 $M_\odot$ of H-rich material with $\epsilon = 0.2$, 2 $M_\odot$ from the He core with $\epsilon = 0.2$, and 2 $M_\odot$ from the O core with $\epsilon = 0.3$. The density of the O component agrees with that derived from the [O I] lines by Spyromilio & Pinto (1991) and Li & McCray (1992). The remaining 30% of the core is occupied by the central Ni bubble, with most of the radioactive material therefore inside the shell. The abundances in the O and He components represent approximately the abundances of these zones in the models by Woosley (1988) and Hashimoto, Nomoto, & Shigeyama (1989). The H component abundances reflect the result of CNO processing from Saio, Nomoto, & Kato (1988). The abundances of the nonprocessed elements are LMC results from Russel & Dopita (1990). Outside the core we add a 10 $M_\odot$ hydrogen envelope with a density profile from the 14E1 model by Shigeyama, Nomoto, & Hashimoto (1988). The γ-ray input in the core is distributed proportionally to the γ-ray optical depths of the three components, while the envelope is exposed to a diluted flux. At 1000 days $\tau_\gamma = 0.06$ for the O core, 0.06 for the He core, 0.11 for the H core, and 0.20 for the H envelope, giving a total $\tau_\gamma = 0.44$, in agreement with that required by the light curve models by Nomoto et al. (1993) and Woosley (1988).

In Paper III we discuss the light curves of the individual lines in detail, and here we only make a few qualitative remarks. The Hα line was discussed in Paper I, and we found an increasing deviation with the observations after day 800.

Including collisional excitation and a self-consistent temperature evolution, the time-dependent effects, especially the long recombination time scale in the envelope, increase the luminosity of this line by an increasing factor with time, giving a satisfactory agreement with observations. Coming mainly from the metal core, the [O I] $\lambda\lambda$6300, 6364 lines are of special interest. Between 400 and 700 days the observed relative contribution to the bolometric luminosity of these lines first falls rapidly. At $\sim$800 days the decay levels off and follows the radioactive curve closely, at a level of $\sim 3 \times 10^{-3}$ of the bolometric luminosity (e.g., Menzies 1991). This behavior is a strong indication of the predicted thermal instability in the O core (Fransson & Chevalier 1987). In our calculations the temperature drop occurs at $\sim$700 days, resulting in a rapid decrease in the relative contribution of the [O I] lines from $\sim$0.1 to $\sim 2 \times 10^{-3}$, shifting most emission from the O core into the far-IR. Collisional excitation by thermal electrons is now unimportant at the low core temperatures (a few hundred K), and a constant flux ratio is a strong indication that nonthermal excitation of the O I ^1D level dominates the [O I] $\lambda\lambda$6300, 6364 production after $\sim$800 days. The change from optical and near-IR transitions to far-IR lines around day 800 is consistent with the observations (e.g., Suntzeff et al. 1992; Bouchet, Danziger, & Lucy 1991), independent of the presence of dust. Dust only thermalizes the radiation further.

Figure 1 shows the bolometric light curve for the standard case, $M(^{57}\mathrm{Ni}) = 3.3 \times 10^{-4}\ M_\odot$ and $M(^{44}\mathrm{Ti}) = 10^{-4}\ M_\odot$, together with the pure ^{56}Ni case, $M(^{57}\mathrm{Ni}) = M(^{44}\mathrm{Ti}) = 0$. To illustrate the departure from steady state, the instantaneous energy input is shown as dashed lines. From the pure ^{56}Ni case we first note the remarkable fact that *even in the absence of a radioactive source, other than* ^{56}Ni, *the light curve levels off after* $\sim$*900 days*, and stays at a level several orders of magnitude above the instantaneous energy input; e.g., at 1500 days the luminosity is 4.7×10^{36} ergs s^{-1}, although the input is only 2.6×10^{35} ergs s^{-1}.

For our standard case Figure 2 (*upper*) shows the individual contributions from the various components, and Figure 2 (*lower*) the bolometric luminosity from each component relative to the energy input. At early stages, the bolometric light curve closely follows the input, but after $\sim$800 days there is a growing departure due to the freeze-out. From Figure 2 (*lower*) it is clear that the increase over the steady state models is mainly a result of emission from the H and He core components, and especially the envelope (§ 2). After 1000 days cooling in the envelope, mainly by fine-structure far-IR [Fe II] lines, is inefficient and the temperature decreases as t^{-2}. At 1500 days $T_e \approx$ 500–1000 K, falling with radius. Due to the higher metallicity, cooling of the O core follows the decay more closely.

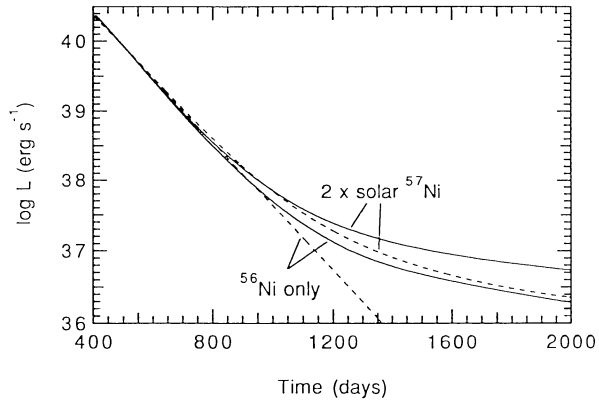

FIG. 1.—The bolometric light curve of SN 1987A for the standard case, $M(^{56}\mathrm{Ni}) = 0.07\ M_\odot$, $M(^{57}\mathrm{Ni}) = 3.3 \times 10^{-3}\ M_\odot$, and $M(^{44}\mathrm{Ti}) = 10^{-4}\ M_\odot$, and pure ^{56}Ni case, $M(^{57}\mathrm{Ni}) = M(^{44}\mathrm{Ti}) = 0$, together with the instantaneous energy input case (*dashed line*).

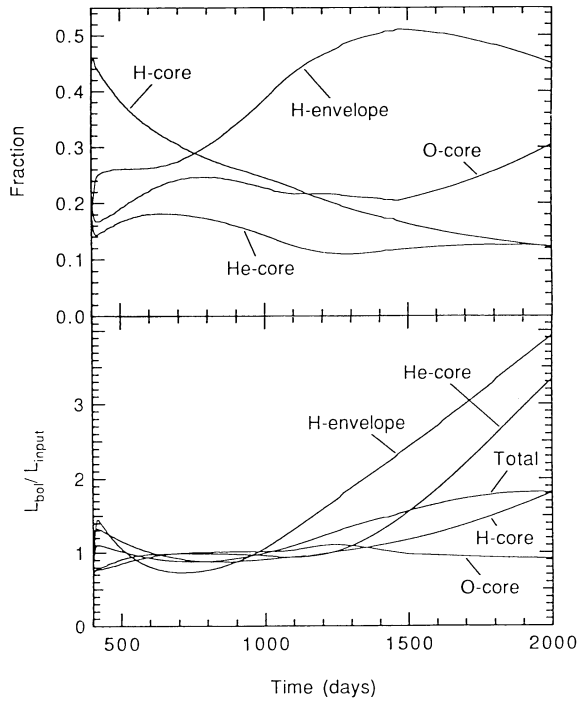

FIG. 2.—Fraction of the total luminosity from the individual components (O core, He core, H core, H envelope) as a function of time for the standard case (*upper*) and the ratio of the emitted luminosity to the energy input (*lower*). Note that the envelope fraction increases from $\sim$25% at 400–600 days, to more than 50% around day 1400.

The observed increase in the line widths after day 800 (Danziger et al. 1991) is consistent with the increasing dominance of the envelope component compared to the core (Fig. 2 [*upper*]). Since freeze-out first occurs in the envelope, it gradually becomes the strongest contributor to the total luminosity.

After day 900 the deviation from the instantaneous input is pronounced, and on day 1500 the steady state luminosity in the standard model is a factor 1.7 lower than in the time-dependent calculation, increasing to a factor 1.9 by day 2000. A quantitative estimate of the amount of ^{57}Co from the light curve can therefore be made only by taking time-dependent effects into account. As the pure ^{56}Ni example shows, our standard model is not at all extreme, rather fairly "conservative."

Having demonstrated the importance of these effects, we can now estimate the required energy input due to ^{57}Co and ^{44}Ti. In Figure 3 we show the bolometric light curves, together with observations and errors from Suntzeff et al. (1991, 1992), for the same model as above, but varying the ^{57}Ni/^{56}Ni ratio. The four cases correspond to no ^{57}Ni (*dashed line*), "solar" ^{57}Ni/^{56}Ni (*dotted line*), 2 times solar (*full line*), and 4 times solar (*dash-dotted line*). In all cases $M(^{44}\mathrm{Ti}) = 10^{-4}\ M_\odot$ except in the case with no ^{57}Ni, where $M(^{44}\mathrm{Ti}) = 0$. It is obvious that the observations show a clear excess over the pure ^{56}Ni curve. On

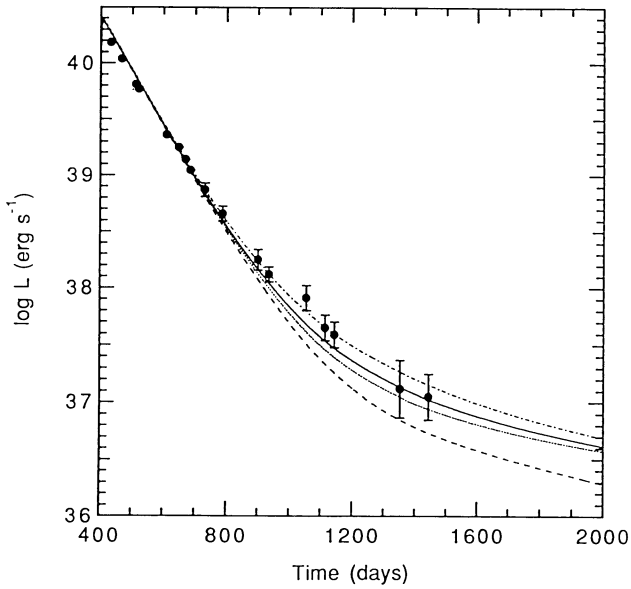

FIG. 3.—Bolometric light curves for different values of the $^{57}Ni/^{56}Ni$ ratio. No ^{57}Ni or ^{44}Ti (*dashed line*), "solar" $^{57}Ni/^{56}Ni$ (*dotted line*), 2 times solar (*full line*), and 4 times solar (*dashed-dotted line*). In the latter three cases, $M(^{44}Ti) = 10^{-4}\ M_{\odot}$. Dots are observations with error bars from Suntzeff et al. (1992).

the other hand, a factor of 4–5 increase in the ^{57}Ni mass, as is indicated from the steady state models (Suntzeff et al. 1992), gives too high a luminosity, especially at the latest points, and a $^{57}Ni/^{56}Ni$ ratio 2 times solar provides the best fit. The difference between the various degrees of ^{57}Ni input is considerably smaller than in a steady state, since time-dependent effects are increasingly important in raising the luminosity for low values of the ^{57}Ni mass. ^{44}Ti becomes important only after $\sim$1500 days, and it is presently difficult to constrain its mass. Later it becomes increasingly dominant because of positron trapping (see above). Most of the energy is then deposited in the metal component, where time dependent effects are least important, input. The emission from the H and He components, however, remain frozen-in (Fig. 2).

4. DISCUSSION

We have shown that the long recombination and cooling time scales after $\sim$800 days may result in a luminosity that can be several times that of the instantaneous energy input due to radioactivity. In spite of a simplified hydrodynamic structure and without serious attempts to vary other parameters than the ^{57}Ni mass, we find good agreement with the observed bolometric light curve using a final $^{57}Fe/^{56}Fe$ ratio equal to $\sim$2 times solar. This value, which is a factor of 2 lower than obtained from steady state models, is consistent with the IR line observations, X-ray, and γ-ray observations, and theoretical models of the nucleosynthesis. A prediction is that there will be an increasing deviation between the steady state luminosity and the observations, which erroneously can be interpreted as either a correspondingly larger ^{57}Co mass or as an extra energy input due to a pulsar. We find no need for the latter up to day 1500. In Chevalier & Fransson (1992) it is argued that a total luminosity of more than $\sim 1 \times 10^{37}$ ergs s^{-1} in terms of ionizing radiation from a pulsar is incompatible with the absence of highly ionized emission from SN 1987A.

The observed fluxes have large errors at late times. The contribution from the far-IR is estimated assuming a dust-thermalized, blackbody form of the spectrum. Since a large fraction of the luminosity then comes from the envelope and H and He core components (Fig. 2), this assumption is doubtful. A spectrum with strong far-IR *lines* can give substantially different results. This will be further discussed in Paper III.

We emphasize that our quantitative results are model dependent, and it is, e.g., not difficult to get even more extreme effects with other structures. The main uncertainty is the hydrodynamic structure, in particular the mixing properties. Although we have tried to model this according to the results of the multidimensional hydrodynamic calculations our structure is simplified. In addition, the hydro models have great uncertainties and difficulties in reproducing, e.g., line profiles and X-ray and γ-ray light curves (e.g., Herant & Benz 1992). However, from the general arguments we have presented it is clear that time-dependent effects must be included in any serious comparison with observations, and this work represents the first attempt to do this.

We are grateful to Roger Chevalier, Alex Dalgarno, John Houck, Peter Lundqvist, and Dick McCray for discussions and comments, and to Silvia Gabi for collecting atomic data and observational material.

REFERENCES

Ahlen, S. P. 1980, Rev. Mod. Phys., 52, 121
Bouchet, P., Danziger, I. J., & Lucy, L. B. 1991, AJ, 102, 1135
Chevalier, R. A. 1992, Nature, 355, 691
Chevalier, R. A., & Fransson, C. 1992, ApJ, 395, 540
Clayton, D. D., Leising, M. D., The, L.-S., Johnson, W. N., & Kurfess, J. D. 1992, ApJ, 399, L141
Danziger, I. J., Bouchet, P., Gouiffes, C., & Lucy, L. B. 1991, in ESO/EIPC Workshop, Supernova 1987A and Other Supernovae, ed. I. J. Danizger & K. Kjär (Garching: ESO), 217
Fransson, C., & Chevalier, R. A. 1987, ApJ, 322, L15
———. 1989, ApJ, 343, 323
Fryxell, B., Müller, E., & Arnett, D. 1991, ApJ, 367, 619
Herant, M., & Benz, W. 1992, ApJ, 387, 294
Hashimoto, M., Nomoto, K., & Shigeyama, T. 1989, A&A, 210, L5
Kozma, C., & Fransson, C. 1992, ApJ, 390, 602 (Paper I)
———. 1993, in preparation (Paper III)
Kumagai, S., Shigeyama, T., Hashimoto, M., & Nomoto, K. 1991, A&A, 243, L13
Kurfess, J. D., et al. 1992, ApJ, 399, L137
Li, H., & McCray, R. 1992, ApJ, 387, 309
Liu, W., Dalgarno, A., & Lepp, S. 1992, ApJ, 396, 679
Menzies, J. W. 1991, in ESO/EIPC Workshop, Supernova 1987A and Other Supernovae, ed. I. J. Danziger & K. Kjär (Garching: ESO), 209
Nomoto, K., Shigeyama, T., Kumagai, S., Yamaoka, H., & Suzuki, T. 1993, in Les Houches, Session LIV, 1990, ed. J. Audouze, S. Bludman, R. Mochkovitch, & J. Zinn-Justin (New York: Elsevier Science Publishers), in press
Russel, S. C., & Dopita, M. A. 1990, ApJS, 74, 93
Saio, H., Nomoto, K., & Kato, M. 1988, Nature, 334, 508
Shigeyama, T., Nomoto, K., & Hashimoto, M. 1988, A&A, 196, 141
Spyromilio, J., & Pinto, P. A. 1991, in ESO/EIPC Workshop, Supernova 1987A and Other Supernovae, ed. I. J. Danziger & K. Kjär (Garching: ESO), 423
Suntzeff, N. B., Philips, M. M., Depoy, D. L., Elias, J. H., & Walker, A. R. 1991, AJ, 102, 1118
———. 1992, ApJ, 384, L33
Varani, G.-F., Meikle, P. S., Spyromilio, J., & Allen, D. A. 1990, MNRAS, 245, 570
Woosley, S. E. 1988, ApJ, 330, 218
Woosley, S. E., & Hoffman, R. D. 1991, ApJ, 368, L31
Woosley, S. E., Pinto, P. A., & Hartmann, D. 1989, ApJ, 346, 395
Woosley, S. E., Pinto, P. A., & Weaver, T. A. 1988, Proc. Astron. Soc. Australia, 7, 355